Uncover the Black Box of Machine Learning Applied to Quantum Problem by an Introspective Learning Architecture

Ce Wang,[1] Hui Zhai,[1, *] and Yi-Zhuang You[2, †]

[1]*Institute for Advanced Study, Tsinghua University, Beijing 10084, China*
[2]*Department of Physics, University of California, San Diego, CA 92093, USA*
(Dated: February 5, 2019)

Recently there is an increasing interest in applying machine learning algorithm to physics problems. These applications provide new platforms to challenge the critical issue of how to uncover the black box of machine learning because there always exists well-defined rules under physics problems. The success of such efforts can offer great promise of discovering new physics from experimental data by artificial intelligence. As a benchmark and a proof-of-principle study that this approach is indeed possible, in this work we design an introspective learning architecture that can automatically develop the concept of the quantum wave function and discover the Schrödinger equation from simulated experimental data of the potential-to-density mappings of a quantum particle. This introspective learning architecture contains a translator and a knowledge distiller. The translator employs a recurrent neural network to learn the potential to density mapping, and the knowledge distiller applies the auto-encoder to extract the essential information and its update law from the hidden layer of the translator, which turns out to be the quantum wave function and the Schrödinger equation. We envision that our introspective learning architecture can enable machine learning to discover new physics in the future.

The ongoing third wave of artificial intelligence has made great achievements in employing neural-network-based machine learning for industry and social applications. Inspired by this great success, machine learning algorithms have also been rapidly applied to various branches physics research, ranging from high-energy and string theory to condensed matter, atomic, molecular and optical physics.[1–18] However, a major challenge is still to uncover the black box of the neural network to understand what kinds of rules has been developed. We consider the machine learning application to physics problems as a better platform to tackle this important challenge. For instance, among different kinds of applications, one type of supervised learning algorithms is to first train the neural network based on labeled experimental data, and then ask the neural network to make predictions. In contrast to the industry and social problems, here both the input and the output data have well-defined physical meaning, and there always exists a clear rule behind the experimental data. The question is whether one can read out the rule by opening up the black box of the neural network, and furthermore, whether the task of reading out the rule can also be carried out by the machine itself. Hence, the most ambitious goal of machine learning physics is not just to perform designated tasks with high accuracy but also to develop novel architectures that allow machine itself to distill the underlying rules from the experimental data.[19, 20]

As a proof-of-concept study that this goal can indeed be achieved, here we consider a single quantum particle moving in a one-dimensional space with certain potential. Suppose we can measure the particle density for each given potential, we supply the machine with the potential profile as the input and the density profile as
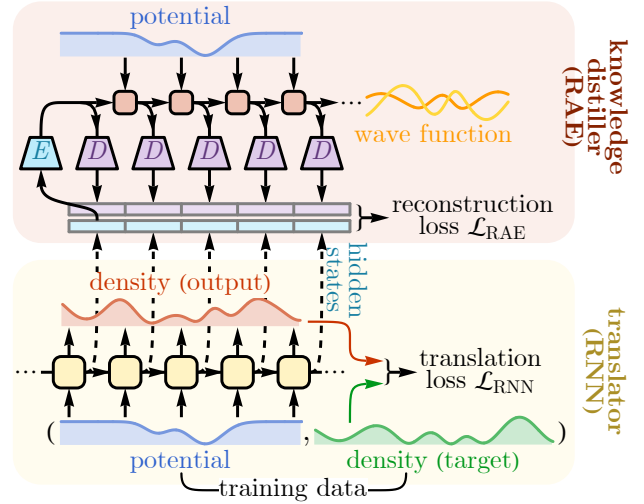

FIG. 1: The architecture of an introspective recurrent neural network, called "the Schrödinger machine". It contains a translator (lower panel) and a knowledge distiller (upper panel). The translator is implemented as a recurrent neural network to perform the task of the potential-to-density mapping. The knowledge distiller compresses the hidden states generated by the translator using a recurrent auto-encoder and extracts the most essential variables in the hidden layer together with its update rule.

the target, and challenge the machine to discover the underlying rule governing the potential-to-density mapping. To this purpose, we develop an introspective learning architecture as shown in Fig. 1 that contains a translator to perform the task of potential-to-density mapping and a knowledge distiller to extract the knowledge behind the mapping. We treat both the potential and den-

sity profiles as sequential data (discretely sampled along the one-dimensional space), then the problem belongs to a broader class of sequence-to-sequence mapping,[21–24] which can be handled by the recurrent neural network (RNN).[25] The RNN has been widely used in natural language processing to translate a sequence of words from the source language to another sequence of words in the target language.[26] Here we construct a novel RNN structure, named "the Taylor RNN", to perform the potential-to-density mapping as a translation task. After training, the RNN can predict the density accurately for any given new potential. As the RNN performs the task, its hidden layer generates a "big data" that should contain the information about the underlying rule governing the potential-to-density mapping, mixed with redundant information.

To extract the essential variables in the hidden layer, we pass the hidden states to a second machine, dubbed as the knowledge distiller. It works on the hidden states of the first machine to compress the information and to extract the underlying rule. The auto-encoder architecture is widely used for information compression.[27, 28] Here we invent an auto-encoder incorporated in a recurrent structure, which we named as the recurrent auto-encoder (RAE). Eventually, we can show that the RAE extracts out that the essential variables in the hidden layers are two real numbers and they can be interpreted as the quantum wave function and its first order derivative. The equation they obeyed is consistent with the Schrödinger equation. In this way, we can conclude that, without any prior knowledge of quantum mechanics, this learning architecture itself can develop the concept of the quantum wave function and discover the Schrödinger equation when it is only provided with experimental data of potential and density pairs. As a consistency check, we also show that if the particle follows classical statistical mechanics, with the same kind of data and similar learning architecture, the Schrödinger equation does not emerge.

The Translator. We discretize the potential $V(x)$ and density profiles $\rho(x)$ along the one-dimensional space and treat them as sequences of real numbers,

$$V_i = V(x_i), \quad \rho_i = \rho(x_i), \tag{1}$$

where $x_i = ai$ are the discrete coordinates for $i = 0, 1, 2, \cdots$, which are evenly distributed along the one-dimensional space with a fixed separation $a = 0.1$. We assume that the potential is always measured with respect to the energy of the particle, such that the particle energy is effectly fixed at zero. We will only consider the case of $V_i < 0$, such that the particle remains in extended states. We apply the RNN architecture to build the translator. In each step, the RNN takes an input V_i from the source sequence, modifies its internal hidden state h_i accordingly, and generates the output ρ'_i based on the hidden state, as illustrated in Fig. 2(a). We adopt
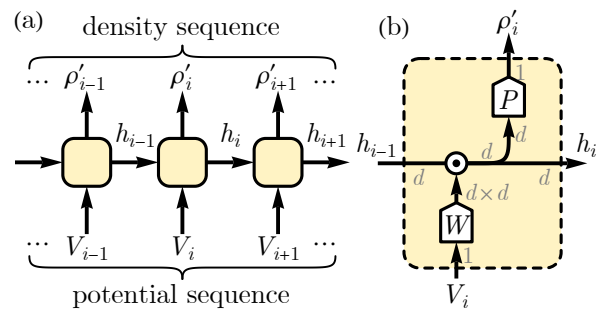

FIG. 2: Architecture of the translator RNN for the potential-to-density mapping. (a) is the global structure and (b) is the network structure within each block. Arrows indicate the direction of information flow. The tensor dimensions are marked out in gray. W and P can be generic functions, although they are modeled by the Taylor expansions in our implementation. The symbol $\odot$ denotes matrix-vector multiplication.

the following update equations

$$h_i = W(V_i) \cdot h_{i-1}, \quad \rho'_i = P(h_i). \tag{2}$$

where both the input $V_i \in \mathbb{R}$ and the output $\rho'_i \in \mathbb{R}$ are scalars and the hidden state $h_i \in \mathbb{R}^d$ is a d-dimensional vector. The hidden state h_i is updated by an input-dependent linear transformation, represented by a $d \times d$ matrix $W(V_i) \in \mathbb{R}^{d \times d}$ multiplied to h_i. The output ρ'_i is generated from the hidden state by a projection map $P(h_i)$. The tensor flow is graphically represented in Fig. 2(b). The output sequence ρ'_i is then compared with the target sequence ρ_i over a window of steps to evaluate the loss function

$$\mathcal{L}_{\mathrm{RNN}} = \sum_{i \in \mathrm{window}} (\rho'_i - \rho_i)^2. \tag{3}$$

How the RNN updates its hidden state and generates output is determined by the functions W and P. In general, W and P could be non-linear functions modeled by feedforward neural networks for instance. However, for our problem, we find it sufficient to model W by a Taylor expansion (to the n_Wth order in V_i) and P by a linear projection,

$$W(V_i) = \sum_{n=0}^{n_W} W^{(n)} V_i^n, \quad P(h_i) = p^{\mathsf{T}} \cdot h_i, \tag{4}$$

where $W^{(n)}$ is the nth order Taylor expansion coefficient matrix (each one is of the dimension $d \times d$) and p is a d-dimensional vector. The elements in $W^{(n)}$ and p are model parameters to be trained to minimize the loss function $\mathcal{L}_{\mathrm{RNN}}$. The training dataset contains pairs of potential and density sequences that serve as parallel corpora to train the RNN translator. They are currently obtained from numerical simulation, but can be
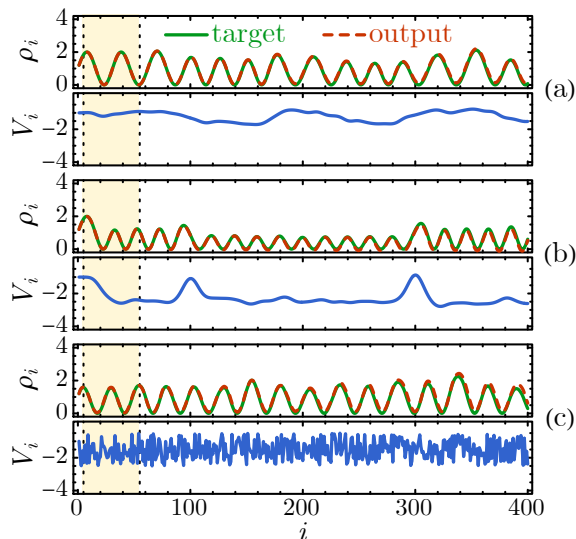
FIG. 3: Typical samples of the RNN output density profiles in comparison with the target density profiles. Three different types of potential profiles are used: (a) a shallow and smooth potential, (b) a deep but smooth potential, (c) a shallow but rough potential. The model is only trained on a small window indicated by the yellow shaded region. The trained RNN can perform the potential-to-density mapping over a much larger range.
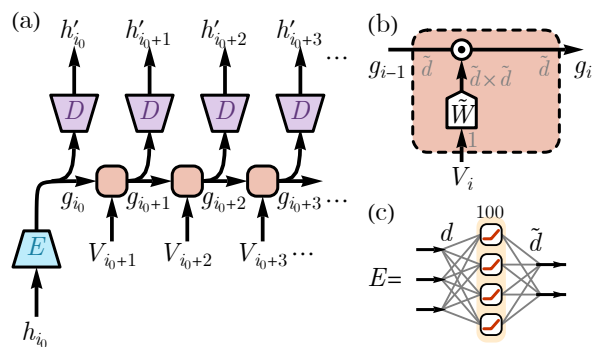

FIG. 4: Architecture of the recurrent auto-encoder. (a) The global structure. (b) The network structure within each recurrent block. (c) The feedforward network of the encoder E. Arrows indicate the direction of information flow. Tensor dimensions are marked out in gray. In (b), $\tilde{W}$ can be a generic function. The symbol $\odot$ denotes matrix-vector multiplication. In (c), we use one hidden layer of 100 dimension, with the ReLU activation. The decoder D has a similar feedforward network in a revered structure as (c).

collected from experiments in future applications, from instance, the quantum gas microscope can detect density of ultracold atoms nearly in their ground state in-situ in the presence of different kind of potentials generated by optical speckles.[29] After minimizing the translator loss $\mathcal{L}_{\mathrm{RNN}}$, the RNN can predict the density profile based on the potential profile.

We build the RNN with the Taylor expansion order $n_W = 2$ and the hidden state dimension up to $d = 6$. We observe that the loss $\mathcal{L}_{\mathrm{RNN}}$ will drop significantly as long as $d \geq 3$. Using the RNN model for the potential-to-density mapping is physically grounded because it respects the translational symmetry of the physical law that governs this mapping. As a result, an immediate advantage of the RNN is to gain spatial scalability, that is, what has been learned over a small system can be readily generalized and applied to larger systems. For instance, as shown in Fig. 3, the RNN is trained over a small window from $i = 5$ to $i = 55$ (the initial 5 outputs are excluded to reduce the sensitivity to initial conditions). After training, the RNN can perform the potential-to-density mapping for a much larger system, from $i = 0$ to $i = 400$. Fig. 3 shows that the RNN output matches nicely with the target density profile on the validation set for different classes of potential profiles, either shallow or deep, and either smooth or rough. This result demonstrates the prediction power of the RNN model.

The Knowledge Distiller. Historically, advances in

physics are often marked by formulating physical phenomena in term of differential equations, such as Newton's law of motion, Maxwell's equation of electromagnetism, and the Schrödinger equation of quantum mechanics. The RNN provides a universal representation of recurrent equations as discretized versions of the differential equations, and therefore the update rules of its hidden state can be interpreted as machine's understanding of the physical laws.[30, 31] Hence, we not only need to find out the essential variables in the hidden states but also need to determine the update rules of these essential variables. Thus, we have to integrate the auto-encoder into the RNN structure, which we called the RAE architecture.

The architecture of the RAE knowledge distiller is illustrated in Fig. 4. The RAE distiller first encodes the hidden state h_{i_0} of the RNN translator at a given step i_0 to the latent variable g_i, and then tries to reconstruct the hidden states h_i for subsequent steps $(i \geq i_0)$ by evolving and decoding the latent variable. The update equations are given by

$$
\begin{aligned}
g_{i_0} &= E(h_{i_0}), \\
g_i &= \tilde{W}(V_i) \cdot g_{i-1}, \quad (i = i_0 + 1, i_0 + 2, \cdots) \quad (5) \\
h'_i &= D(g_i), \quad (i = i_0, i_0 + 1, i_0 + 2, \cdots)
\end{aligned}
$$

where E and D represent the encoder and decoder maps respectively. Here the RAE hidden state $g_i \in \mathbb{R}^{\tilde{d}}$ is updated by an linear transformation $\tilde{W}(V_i)$ that will still depend on the input potential sequence V_i, as illustrated in Fig. 4(b). The encoder and the decoder are implemented by feedforward networks as shown in Fig. 4(c).
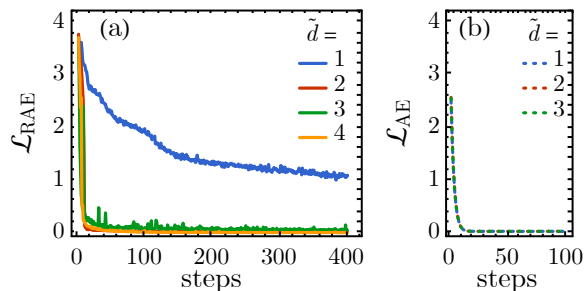
FIG. 5: (a) The RAE reconstruction loss $\mathcal{L}_{\mathrm{RAE}}$ v.s. the training steps for the quantum case. Different curves are for different RAE hidden state dimensions $\tilde{d}$. $\tilde{d} = 2$ turns out to be the minimal $\tilde{d}$ without sacrificing the reconstruction loss. (b) The AE reconstruction loss $\mathcal{L}_{\mathrm{AE}}$ v.s. training steps for the classical thermal gas. The vanishing $\mathcal{L}_{\mathrm{AE}}$ implies that there is no need to pass any variable along the sequence in this case.

The RAE is trained to minimize the reconstruction loss

$$\mathcal{L}_{\mathrm{RAE}} = \sum_{i \in \mathrm{window}} (h'_i - h_i)^2. \tag{6}$$

It is important that the RAE (knowledge distiller) hidden state g_i has a smaller dimension $\tilde{d}$ compared to the dimension d of the RNN (translator) hidden state h_i, therefore it can enforce an information bottleneck that only allows the vital information to be passed down in g_i. Furthermore, instead of using a single auto-encoder to compress the hidden state at each step independently, the RAE connects a series of decoders together by a recurrent neural network. This design is to ensure that the latent representation g_i remains coherent among a series of steps and contains the key variables that should be passed down along the sequence. A similar RAE architecture was proposed in Ref. 32 and recently redesigned in Ref. 19 to enable AI scientific discovery on sequential data. In this way, the RAE compresses the original RNN to a more compact RNN capturing the most essential information and its induced update rules.

As shown in Fig. 5(a), we find that the reconstruction loss $\mathcal{L}_{\mathrm{RAE}}$ of the RAE increases dramatically only when its hidden state dimension $\tilde{d}$ is squeezed below two (i.e. $\tilde{d} < 2$), implying that the key feature can be stored in a two-component real vector (i.e. $\tilde{d} = 2$) in the most parsimonious manner, as $g_i = (g_{i,1}, g_{i,2})$. Here we show that g_i in fact represent the quantum wave function and its first order derivation. The evidences are two fold:

First, we try to use the trained RNN to predict the density with a constant potential V, the result of which should be $\cos^2(kx_i)$ with $k = \sqrt{-V}$ being the momentum. Indeed it is the case as shown in Fig. 6. If $g_{i,1}$ and $g_{i,2}$ are the wave function and its derivative, it should be $\cos(kx_i)$ and $\sin(kx_i)$, respectively, whose periods are twice of the period of ρ_i with phases shifted by $\pi/2$ relative to each other. As shown in Fig. 6, g_i indeed displays
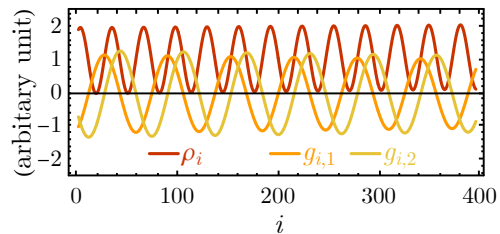
FIG. 6: The RNN output density profile ρ_i and the RAE hidden state $g_i = (g_{i,1}, g_{i,2})$ for a constant potential $V_i = 1$. It shows that the periodicity of g_i is twice of ρ_i.

the periodicity doubling and the relative phase shift.

Second, we open up the recurrent block of the RAE to extract the update rules for g_i, which is machine's formulation of the physical rules. The update rules are encoded in the transformation matrix $\tilde{W}(V_i) = \sum_{n=0}^{n_W} \tilde{W}^{(n)} V_i^n$, which are parameterized by the Taylor expansion coefficient matrices $\tilde{W}^{(n)}$. To connect this formulation to the Schrödinger equation we familiar with, we notice that this mapping is invariant under a linear transformation $M \in \mathrm{GL}(2, \mathbb{R})$ applied to all $\tilde{W}^{(n)}$. We find that it is always possible to find a proper linear transformation that can *simultaneously* bring all $\tilde{W}^{(n)}$ to the following form

$$\begin{aligned} M^{-1}\tilde{W}^{(0)}M &= \begin{bmatrix} 0.9993 & 0.1007 \\ 0.0013 & 0.9987 \end{bmatrix} \approx \begin{bmatrix} 1 & a \\ 0 & 1 \end{bmatrix}, \\ M^{-1}\tilde{W}^{(1)}M &= \begin{bmatrix} 0.0067 & 0.0004 \\ 0.1001 & 0.0024 \end{bmatrix} \approx \begin{bmatrix} 0 & 0 \\ a & 0 \end{bmatrix}. \end{aligned} \tag{7}$$

Here the numerical matrix elements are what we obtained from a particular instance of the trained RAE. They can be associated to the lattice constant a to the leading order given that $a = 0.1$, and we have also verified that they scale correctly with a as proposed. The result in Eq. (7) points to the following difference equation

$$\begin{bmatrix} g_{i+1,1} \\ g_{i+1,2} \end{bmatrix} = \begin{bmatrix} 1 & a \\ aV(x) & 1 \end{bmatrix} \begin{bmatrix} g_{i,1} \\ g_{i,2} \end{bmatrix}. \tag{8}$$

If we interpret $g_{i,1}$ as the quantum wave function $\psi(x_i)$ and $g_{i,2}$ as its first order derivative $\partial_x \psi(x_i)$, Eq. (8) corresponds to a discrete version of the Schrödinger equation $\partial_x^2 \psi(x) = V(x)\psi(x)$ as the particle energy was taken to be zero.

Finally, as a consistency check, we train the same introspective recurrent neural network on the potential and density data of the high-temperature thermal gas following $\rho_i \propto e^{-\beta V_i}$ at a fixed inverse temperature β. In this case, we can even reduce the RAE to an auto-encoder (AE) without sacrificing the reconstruction loss $\mathcal{L}_{\mathrm{AE}}$. As shown in Fig. 5(b), the $\mathcal{L}_{\mathrm{AE}}$ remains vanishing for any $\tilde{d}$, implying that there is no need to pass any variable along the sequence and hence the Schödinger equation will not emerge for thermal gas.

Conclusion. To conclude, we design the architecture that combines a task machine directly learning the experimental data and an introspective machine working on the neural activations of the task machine. The separation of the task machine from the introspective machine effectively isolates the knowledge distillation from affecting the task performance, such that the whole system can simultaneously improve the task performance and approach the parsimonious limit of knowledge representation, without trading off between one another. Here we show that this architecture can discover the Schrödinger equation from the potential-to-density data. Therefore we name it as the "Schrödinger machine". We envision that the same architecture can be generally applied to other machine learning applications to physics problems and enable machine learning to discover new physics in the future.

Besides, there are another few points worth highlighting in this work. First, although the use of Taylor expansion for the non-linear functions in our RNN is not essential and can be replaced by neural network models, it has the advantage of being analytical tractability which makes it easier to understand how the RNN works. Second, the potential-to-density mapping is also an essential component in the density functional theory, known as the Kohn-Sham mapping.[33] The existing machine learning solutions for this task include the kernel method and the convolutional neural network approach.[16, 17, 34–36] The RNN approach introduced here has the advantage of being spatially scalable without retraining, which could find potential applications in boosting the density functional calculation and material search. Thirdly, we invent a model that incorporates the auto-encoder with the recurrent neural network, which can find a compact representation of the entire RNN model. This algorithm can find its application in other occasions of model compression and knowledge transfer.

———————

* Electronic address: hzhai@tsinghua.edu.cn
† Electronic address: yzyou@physics.ucsd.edu

[1] J. Carifio, J. Halverson, D. Krioukov, and B. D. Nelson, Journal of High Energy Physics **9**, 157 (2017), 1707.00655.
[2] J. Liu, Journal of High Energy Physics **12**, 149 (2017), 1707.02800.
[3] Y.-N. Wang and Z. Zhang, Journal of High Energy Physics **8**, 9 (2018), 1804.07296.
[4] M. Koch-Janusz and Z. Ringel, Nature Physics **14**, 578 (2018), 1704.06279.
[5] Y.-Z. You, Z. Yang, and X.-L. Qi, Phys. Rev. B **97**, 045153 (2018), 1709.01223.
[6] K. Hashimoto, S. Sugishita, A. Tanaka, and A. Tomiya, ArXiv e-prints (2018), 1802.08313.
[7] G. Torlai and R. G. Melko, Phys. Rev. B **94**, 165134 (2016), 1606.02718.
[8] L. Wang, Phys. Rev. B **94**, 195105 (2016).
[9] J. Carrasquilla and R. G. Melko, Nature Physics **13**, 431 (2017), 1605.01735.
[10] E. P. L. van Nieuwenburg, Y.-H. Liu, and S. D. Huber, Nature Physics **13**, 435 (2017), 1610.02048.
[11] Y. Zhang and E.-A. Kim, Physical Review Letters **118**, 216401 (2017), 1611.01518.
[12] C. Wang and H. Zhai, Phys. Rev. B **96**, 144432 (2017), 1706.07977.
[13] C. Wang and H. Zhai, Frontiers of Physics **13**, 130507 (2018), 1803.01205.
[14] P. Zhang, H. Shen, and H. Zhai, Physical Review Letters **120**, 066401 (2018), 1708.09401.
[15] G. Torlai, G. Mazzola, J. Carrasquilla, M. Troyer, R. Melko, and G. Carleo, Nature Physics **14**, 447 (2018).
[16] J. C. Snyder, M. Rupp, K. Hansen, K.-R. Müller, and K. Burke, Phys. Rev. Lett. **108**, 253002 (2012).
[17] F. Brockherde, L. Vogt, L. Li, M. E. Tuckerman, K. Burke, and K.-R. Müller, Nature Communications **8**, 872 (2017).
[18] K. Mills, M. Spanner, and I. Tamblyn, Phys. Rev. A **96**, 042113 (2017).
[19] R. Iten, T. Metger, H. Wilming, L. del Rio, and R. Renner, ArXiv e-prints (2018), 1807.10300.
[20] T. Wu and M. Tegmark, arXiv e-prints arXiv:1810.10525 (2018), 1810.10525.
[21] N. Kalchbrenner and P. Blunsom, in *Proceedings of the 2013 Conference on Empirical Methods in Natural Language Processing* (Association for Computational Linguistics, 2013), pp. 1700–1709.
[22] I. Sutskever, O. Vinyals, and Q. V. Le, in *Advances in Neural Information Processing Systems 27*, edited by Z. Ghahramani, M. Welling, C. Cortes, N. D. Lawrence, and K. Q. Weinberger (Curran Associates, Inc., 2014), pp. 3104–3112.
[23] K. Cho, B. van Merrienboer, C. Gulcehre, D. Bahdanau, F. Bougares, H. Schwenk, and Y. Bengio, ArXiv e-prints (2014), 1406.1078.
[24] D. Bahdanau, K. Cho, and Y. Bengio, ArXiv e-prints (2014), 1409.0473.
[25] I. Goodfellow, Y. Bengio, and A. Courville, *Deep Learning* (MIT Press, 2016).
[26] G. Neubig (2017), 1703.01619.
[27] Y. Bengio, A. Courville, and P. Vincent, IEEE Transactions on Pattern Analysis and Machine Intelligence **35**, 1798 (2013), ISSN 2160-9292.
[28] D. P. Kingma and M. Welling, arXiv preprint arXiv:1312.6114 (2013).
[29] J. E. Lye, L. Fallani, M. Modugno, D. S. Wiersma, C. Fort, and M. Inguscio, Phys. Rev. Lett. **95**, 070401 (2005).
[30] C. Ma, J. Wang, and W. E, ArXiv e-prints (2018), 1808.04258.
[31] L. Banchi, E. Grant, A. Rocchetto, and S. Severini, ArXiv e-prints (2018), 1808.01374.
[32] P. Mirowski, M. Ranzato, and Y. LeCun, in *Proceedings of the NIPS 2010 Workshop on Deep Learning* (2010), vol. 2.
[33] W. Kohn and L. J. Sham, Physical review **140**, A1133 (1965).

[34] L. Li, J. C. Snyder, I. M. Pelaschier, J. Huang, U.-N. Niranjan, P. Duncan, M. Rupp, K.-R. Müller, and K. Burke, ArXiv e-prints (2014), 1404.1333.

[35] L. Li, T. E. Baker, S. R. White, and K. Burke, Phys. Rev. B **94**, 245129 (2016).

[36] Y. Khoo, J. Lu, and L. Ying, ArXiv e-prints (2017), 1707.03351.

<div align="center">SUPPLEMENTARY MATERIAL</div>

Trackable Limit of RNN Translator

The RNN translator may not be able to formulate physical laws in the most parsimonious language. The hidden state of the RNN may contain redundant information. In fact, there is an analytically tractable limit where we can explicitly demonstrate this possibility. For example, the RNN may tried to capture the differential equation for the density profile directly, instead of that for the quantum wave function. To simplify the analysis, let us take $\hbar^2/(2ma^2)$ as our energy unit and define the potential energy with respect to the single-particle energy level, then the Schrödinger equation for the BEC wave function $\psi(x)$ takes a rather simple form of $\partial_x^2 \psi(x) = V(x)\psi(x)$. However, in terms of the density profile $\rho(x) = |\psi(x)|^2$, the Schrödinger equation implies

$$\partial_x \begin{bmatrix} \rho(x) \\ \eta(x) \\ \xi(x) \end{bmatrix} = \begin{bmatrix} 0 & 2 & 0 \\ V(x) & 0 & 1 \\ 0 & 2V(x) & 0 \end{bmatrix} \begin{bmatrix} \rho(x) \\ \eta(x) \\ \xi(x) \end{bmatrix}, \qquad (9)$$

where $\eta(x) = \mathrm{Re}\,\psi^*(x)\partial_x\psi(x)$ and $\xi(x) = |\partial_x\psi(x)|^2$ are two other real profiles that combine with $\rho(x)$ to form a system of linear differential equations. The recurrent rule for such a system lies within the description power of our RNN architecture. If the RNN choose to identify its hidden state as $h_i = [\rho(x_i), \eta(x_i), \xi(x_i)]^\intercal$, the following parameters will allow it to model Eq. (9) with good accuracy to the first order in a:

$$W^{(0)} = \begin{bmatrix} 1 & 2a & 0 \\ 0 & 1 & a \\ 0 & 0 & 1 \end{bmatrix}, W^{(1)} = \begin{bmatrix} 0 & 0 & 0 \\ a & 0 & 0 \\ 0 & 2a & 0 \end{bmatrix}, p = \begin{bmatrix} 1 \\ 0 \\ 0 \end{bmatrix}. \quad (10)$$

This theoretical construction at least provides us a base RNN that demonstrates why the proposed architecture in Eq. (2) could work in principle. The performance can be further improved by relaxing the parameters from this idea limit or by enlarging the hidden state dimension d.
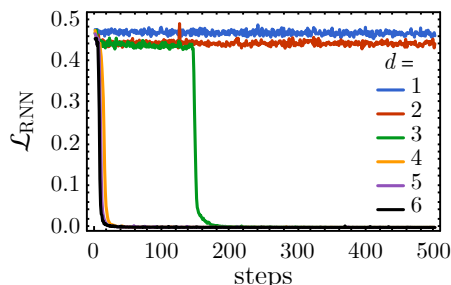

FIG. 7: The RNN translator loss $\mathcal{L}_{\mathrm{RNN}}$ (on the test data set) v.s. the training steps, for different hidden state dimensions $d = 1, 2, \cdots, 6$. The RNN is only able to master the potential-to-density mapping for $d \geq 3$.

However, what is the minimum hidden state dimension d (in terms of real variables) for the RNN to function well in the potential-to-density mapping? Can the RNN discover that the quantum wave function $\psi(x)$ could provide a more parsimonious description, which only requires two real variables $\mathrm{Re}\,\psi(x)$ and $\mathrm{Im}\,\psi(x)$ to parameterize? To answer these questions, we train the RNN translator under different hidden state dimensions d. As shown in Fig. 7, we observe that the loss $\mathcal{L}_{\mathrm{RNN}}$ only drop significantly if $d \geq 3$, implying that the RNN was unable to realize the more efficient ($d = 2$) wave function description. For the $d = 3$ case, as we read out the hidden states h_i at each step, we found that they indeed correspond to the vector $[\rho(x_i), \eta(x_i), \xi(x_i)]^\intercal$ up to specific linear transformation (depending on the random initialization of the model parameters), confirming that the RNN indeed works like the base model Eq. (10). From this example, we see that the RNN could develop legitimate and predictive rules of physics, such as Eq. (9), from the observation data. It tends to work directly with the variables present in the observation data to get the job done. Sometimes the rules it found can work well enough that the RNN may not have the motivation to develop higher-level concepts like quantum wave functions.

Method

In this section, we elaborate on the details of our training process. For the RNN based on Taylor expansion, we cut off the expansion at power $n_W = 2$, and consider the hidden space dimension d from 1 to 6. Taking $d = 6$ as an example, the initial $h_0 = (1, 1, 1, 1, 1, 1)$ and the vector $p = (p_1, 0, 0, 0, 0, 0)$ without loss of generality, the parameter p_1 is set to be 1 initially. We initialize the coefficient matrices $W^{(n)}$ to

$$
\begin{aligned}
W^{(0)} &= \mathbf{1}_{d\times d} + \frac{0.01}{d}\mathsf{randn}_{d\times d},\ (\text{for } n = 0) \\
W^{(n)} &= \frac{0.01}{d}\mathsf{randn}_{d\times d},\ (\text{for } n > 0)
\end{aligned}
\tag{11}
$$

where $\mathbf{1}_{d\times d}$ stands for the $d \times d$ dimensional identity matrix and $\mathsf{randn}_{d\times d}$ stands for the $d\times d$ dimensional random matrix whose elements follow independent Gaussian distributions (with unit variance and zero mean). The training method we use is ADAM method with learning rate 0.0002, the mini-batch size is 5. The training window is from $i = 5$ to $i = 55$.

For the RAE network, the encoder is a feedforward network of $d = 6 \rightarrow 100 \rightarrow \mathsf{ramp} \rightarrow \tilde{d}$ structure and the decoder is also a feedforward network of $\tilde{d} \rightarrow 100 \rightarrow \mathsf{ramp} \rightarrow d = 6$ structure. The training method we use is ADAM method with learning rate 0.001, the mini-batch size is 5. The training window is from $i = 5$ to $i = 60$.

Data Acquisition

The data for training RNN are generated by solving the "simplified" Schrödinger equation in 1d

$$V(x)\psi(x) = \partial_x^2 \psi(x). \tag{12}$$

x labels the position in 1D. The potential begins at $x = 0$ and $V(x_i) = V_i$ for $x_i \equiv ia$ where $a = 0.1$ is a short range cut-off. We define $k_i = \sqrt{-V_i}$, then the wave function should take the form of $\psi(x) = A_i \sin(k_i x) + B_i \cos(k_i x)$ for $x_i \leq x < x_{i+1}$. Matching the wave function and its derivative will give the relations,

$$
\begin{aligned}
k_{i+1} A_{i+1} =& A_i (k_{i+1} \sin(k_i x_i) \sin(k_{i+1} x_i) \\
& + k_i \cos(k_i x_i) \cos(k_{i+1} x_i)) \\
& + B_i (k_{i+1} \cos(k_i x_i) \sin(k_{i+1} x_i) \\
& - k_i \sin(k_i x_i) \cos(k_{i+1} x_i))
\end{aligned} \tag{13}
$$

$$
\begin{aligned}
k_{i+1} B_{i+1} =& B_i (k_i \sin(k_i x_i) \sin(k_{i+1} x_i) \\
& + k_{i+1} \cos(k_i x_i) \cos(k_{i+1} x_i)) \\
& + A_i (k_{i+1} \sin(k_i x_i) \cos(k_{i+1} x_i) \\
& - k_i \cos(k_i x_i) \sin(k_{i+1} x_i))
\end{aligned} \tag{14}
$$

With these relations, we can solve all the A_i, B_i starting from a fixed initial condition $A_0 = 1, B_0 = 1$, hence we can construct the wave function $\psi(x)$. Finally the density at x_i is given by

$$\rho_i = \psi(x_i)^2. \tag{15}$$

In summary, each data is generated in following steps:

1. Set $V_1 = -1$ and the rest $V_i = -2 * \mathsf{rand} - R$. Where rand is a random number uniformly distributed in $[0,1]$ for each V_i, and R is a random number uniformly distributed in $[0,1]$ which is the same for each sequence. We use R to randomly shift the energy scale for each data.

2. Make the potential V_i more smooth by performing a flatten operation, $V_{i+1} = 0.5 * (V_i + V_{i+1})$, for q times, where q is a random integer between 1 and 20.

3. Get the density sequence ρ_i for this potential by solving Eq.13, Eq.14 and using Eq.15.

In practice, we collect 15000 data, 10000 of them used for training and 5000 of them are used for validation.

While the potential data for RAE are generated in the same way as for RNN, and the hidden state h_i are collected by evolving the trained RNN. We collect 15000 data, 10000 of them are used for training and 5000 of them are used for the validation.